Origin of the Structural and Magnetic Anomalies of the Layered Compound $SrFeO_2$: A Density Functional Investigation

H. J. Xiang and Su-Huai Wei
National Renewable Energy Laboratory, Golden, Colorado 80401, USA

M.-H. Whangbo
Department of Chemistry, North Carolina State University, Raleigh, North Carolina 27695-8204, USA
(Received 31 December 2007; published 25 April 2008)

The structural and magnetic anomaly of the layered compound $SrFeO_2$ are examined by first-principles density functional calculations and Monte Carlo simulations. The down-spin Fe $3d$ electron occupies the d_{z^2} level rather than the degenerate (d_{xz}, d_{yz}) levels, which explains the absence of a Jahn-Teller instability, the easy ab-plane magnetic anisotropy, and the observed three-dimensional (0.5, 0.5, 0.5) antiferromagnetic order. Monte Carlo simulations show that the strong interlayer spin exchange is essential for the high Néel temperature.

DOI: 10.1103/PhysRevLett.100.167207 PACS numbers: 75.30.Gw, 64.60.De, 71.20.−b, 75.50.Ee

Perovskite oxides have attracted considerable interest due to their extensive applications in a number of technological areas. Among them, $SrFeO_{3-x}$ and its related iron perovskite oxides exhibit fast oxygen transport and high electron conductivity even at low temperatures [1–5]. It had previously been believed that the end member phases for these compounds are the orthorhombic brownmillerite $SrFeO_{2.5}$ ($x = 0.5$) and the cubic perovskite $SrFeO_3$ ($x = 0$). Very recently, the range of x was extended to $x = 1$ by Tsujimoto *et al.*, who discovered that $SrFeO_2$ has planar FeO_2 layers made up of corner-sharing FeO_4 squares with high-spin Fe^{2+} (d^6) ions, separated by Sr^{2+} ions [6,7].

$SrFeO_2$ exhibits interesting and apparently puzzling physical properties [6]. First, if the lone down-spin electron of a high-spin Fe^{2+} (d^6) ion at square-planar site occupies the degenerate (d_{xz}, d_{yz}) orbitals, as expected by the crystal field theory [8], $SrFeO_2$ should be subject to orbital ordering or Jahn-Teller distortion when the temperature is lowered [9]. However, $SrFeO_2$ shows no structural instability and maintains the space group $P4/mmm$ down to 4.2 K [6]. Second, $SrFeO_2$ displays a three-dimensional (3D) antiferromagnetic (AFM) order with a very high Néel temperature ($T_N = 473$ K) [6], which is even higher than that (~ 200 K) of FeO with a 3D structure. Such a high 3D AFM ordering temperature in a layered system is remarkable and unexpected, because T_N usually decreases drastically when the dimensionality decreases. Third, the powder neutron diffraction study shows that the magnetic moments are perpendicular to the c axis (the local z axis) [6], which is not consistent with the occupation of the (d_{xz}, d_{yz}) orbitals with three electrons [10].

To probe the causes for these apparently anomalous structural and magnetic properties in $SrFeO_2$, we examined the magnetic properties of $SrFeO_2$ by performing density functional theory (DFT) band structure and total energy calculations to evaluate its spin exchange interactions and performing Monte Carlo (MC) simulations to calculate the Néel temperature using the extracted spin exchange parameters. We show that the down-spin Fe $3d$ electron in $SrFeO_2$ occupies the nondegenerate d_{z^2} level rather than the degenerate (d_{xz}, d_{yz}) levels, which explains the absence of Jahn-Teller instability, the occurrence of the easy ab-plane magnetic anisotropy as well as the strongly AFM coupling between the interlayer and intralayer nearest-neighbor (NN) Fe^{2+} ions thereby giving rise to the observed 3D (0.5, 0.5, 0.5) AFM order in $SrFeO_2$. MC simulations of specific heat show that the strong interlayer spin exchange is essential for the high Néel temperature. Similar results are also found for the hypothetical isostructural compounds $CaFeO_2$ and $BaFeO_2$.

Our first-principles spin-polarized DFT calculations for $MFeO_2$ (M = Ca, Sr, Ba) were performed on the basis of the projector augmented wave method [11] encoded in the Vienna *ab initio* simulation package [12] using the local density approximation [13] and the plane-wave cutoff energy of 400 eV. To properly describe the strong electron correlation associated with the Fe $3d$ states, the LDA plus on-site repulsion U method (LDA + U) was employed [14]. In the following, we report only those results obtained with $U = 4.6$ eV and $J = 0$ eV on Fe [15], but the use of other U values between 3–6 leads to qualitatively the same results.

$SrFeO_2$ adopts the $P4/mmm$ space group with $a = 3.985$ Å and $c = 3.458$ Å at 10 K [6]. As shown in Fig. 1, the FeO_2 layers separated by Sr^{2+} ions are stacked along the c axis. As a first step to discuss the magnetic properties of $SrFeO_2$, the electronic structure of $SrFeO_2$ calculated for its ferromagnetic (FM) state [$\mathbf{q} = (0.0, 0.0, 0.0)$] is presented in Fig. 2. The band dispersion relations of Fig. 2(a) show that the FM state is metallic because the top portion of the up-spin valence bands (an O p and Fe d state) is above the bottom portion of the up-spin conduc-

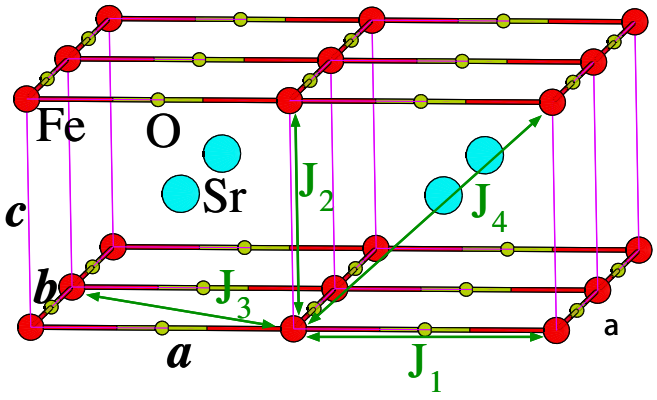

FIG. 1 (color online). Perspective view of the tetragonal structure of $SrFeO_2$. The large, middle, and small spheres represent the Sr, Fe, and O ions, respectively. The spin exchange paths J_1, J_2, J_3, and J_4 are also indicated.

tion bands (a Fe p and Sr d state) at R (0.5, 0.5, 0.5) point. The plots of the density of states (DOS) and the partial DOS (PDOS) in Fig. 2(b) reveal that there is a strong hybridization between the O $2p$ and Fe $3d$ states in the valence bands. Further analysis shows that the largest coupling occurs at R point between Fe $d_{x^2-y^2}$ orbital and O p_x, p_y orbitals. When the PDOS plots of the Fe and O atoms in Fig. 2(b) are compared with those of the Fe $3d$ states in Fig. 2(c), it is seen that the up-spin bands have Fe $3d$ energy levels below the O $2p$ state, whereas the down-spin Fe $3d$ bands is above. This reflects the large exchange splitting of the Fe $3d$ levels, which is responsible for the high-spin state of the Fe^{2+} ion. It is important to note from Fig. 2 that the occupied down-spin state has the d_{z^2} character, not the doubly-degenerate (d_{xz}, d_{yz}) character as expected from crystal field theory for the D_{4h} point symmetry [6,8]. This is because in the layered structure, the energy of the d_{z^2} state is significantly decreased due to the reduced Coloumb repulsion. Because the d_{z^2} is nondegenerate, no Jahn-Teller type distortion is expected for $SrFeO_2$, as found experimentally [6].

To determine the magnetic ground state and discuss the magnetic properties of $SrFeO_2$, we considered four more ordered spin states besides the FM state, namely, the AF1 state with $\mathbf{q} = (0.5, 0.5, 0.5)$, the AF2 state with $\mathbf{q} = (0.0, 0.0, 0.5)$, the AF3 state with $\mathbf{q} = (0.5, 0.5, 0.0)$, and the AF4 state with $\mathbf{q} = (0.5, 0.0, 0.5)$. The experimentally observed AFM structure is AF1. Our LDA + U calculations show that all the AFM states are lower in energy than the FM state, and the AF1 state is the ground state, in good agreement with experiment [6]. These results are consistent with the facts that in the high-spin (d^6) configuration, there is no partially occupied d state to stabilize the FM phase [16]. The total DOS and PDOS plots presented in Fig. 3 show that $SrFeO_2$ in the AF1 phase has a band gap as expected for this magnetic semiconductor. Comparing to the electronic band structures of the FM phase, the band structure of the AF1 phase exhibit an important difference;

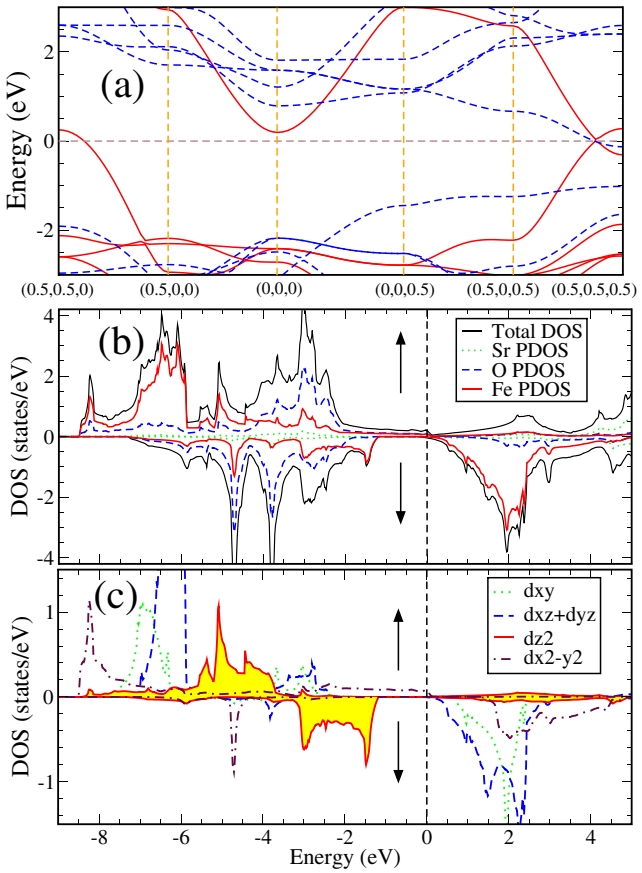

FIG. 2 (color online). Electronic structure calculated for the FM state of $SrFeO_2$: (a) Dispersion relations of the up-spin and down-spin bands (solid and dashed lines, respectively) in the vicinity of the Fermi level. (b) Total DOS and PDOS plots for the Sr, Fe, and O atom contributions. (c) PDOS plots for the Fe $3d$ orbitals, where the PDOS for the Fe d_{z^2} orbital was highlighted by shading.

overall, the d bands are narrower in the AF1 than in the FM state. In particular, the up-spin $d_{x^2-y^2}$ band has a significantly narrower bandwidth in the AF1 state. This observation is readily accounted for by considering a spin-1/2 square-net lattice with one magnetic orbital per site, the hopping integral t between adjacent sites and the on-site repulsion U. For the FM arrangement of the spins, the up-spin (or down-spin) states of adjacent sites are identical in energy and the interaction energy between them is t, so the widths of the up-spin and down-spin bands are proportional to t. For the AFM arrangement of spins, the up-spin (or down-spin) states of adjacent sites differ in energy by U and the interaction energy between them is t^2/U, so the widths of the up-spin and down-spin bands are proportional to t^2/U. Since $t \gg t^2/U$ for usual magnetic solids, the width of the electronic energy band is much wider for the FM state than for the AFM state.

To extract the values of the four spin exchange parameters J_1, J_2, J_3, and J_4 (see Fig. 1), we map the relative energies of the five ordered spin states (i.e., FM, AF1, AF2,

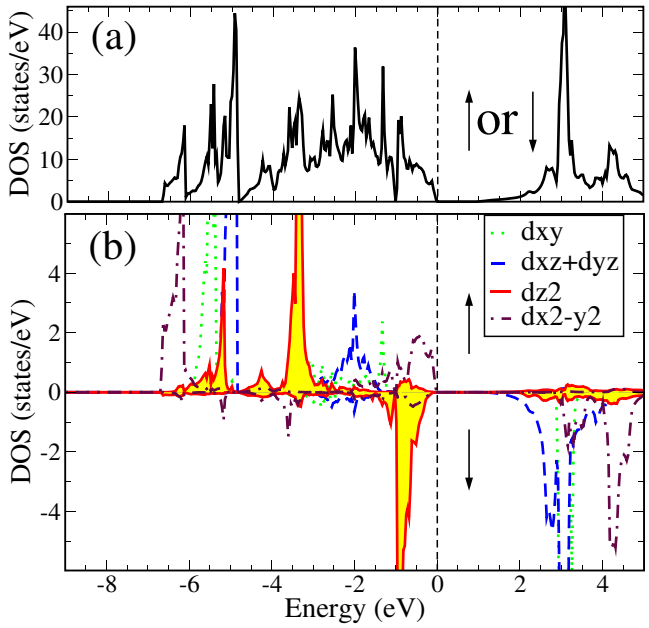

FIG. 3 (color online). Electronic structure calculated for the AF1 state of $SrFeO_2$: (a) Total DOS plot, which is identical for the up-spin and down-spin bands. (b) PDOS plots calculated for the Fe $3d$ orbitals, where the shaded regions refer to the Fe $3d_{z^2}$ orbital contributions.

AF3, and AF4) obtained from the LDA + U calculations onto the corresponding energies given by the Heisenberg spin Hamiltonian made up of the four spin exchange parameters. This mapping analysis was carried out as described in Ref. [17]. The obtained exchange parameters are summarized in Table I. The intralayer NN spin exchange J_1 is quite strong, which is due to the strong 180° Fe-O-Fe superexchange between the $d_{x^2-y^2}$ orbitals mediated by O p_x and p_y orbitals [18,19]. The interlayer NN spin exchange J_2 is strongly AFM and is weaker than J_1 only by a factor of ~3. The interlayer spin exchange J_2 originates from the direct through-space overlap between the d_{xz}/d_{yz} orbitals of Fe.

To account for the observed anisotropic magnetic property of $SrFeO_2$, we carried out LDA + U calculations for the FM state by including spin-orbit coupling (SOC) interactions. These LDA + U + SOC calculations show that the state with the spin moments parallel to the ab plane is more stable than the state with the spin moments parallel to the c axis by 4 meV/Fe, while the calculated orbital moment is 0.22 μ_B for the $\perp c$ spin arrangement, and 0.01 μ_B for the $\| c$ spin arrangement. This easy ab-plane anisotropy, which is in accord with experiment [6], can be explained by analyzing the SOC Hamiltonian [20]. Since the up-spin and down-spin d bands are well separated due to the large exchange splitting, one can neglect interactions between the up-spin and down-spin states under the SOC. With θ and ϕ as the zenith and azimuth angles of the magnetization in the direction $\mathbf{n}(\theta, \phi)$, the spin-conserving term of the $\lambda\hat{\mathbf{L}} \cdot \hat{\mathbf{S}}$ operator ($\lambda < 0$ for Fe^{2+}) is given by [20,21]

$$\lambda \hat{S}_n(\hat{L}_z \cos\theta + \tfrac{1}{2}\hat{L}_+ e^{-i\phi} \sin\theta + \tfrac{1}{2}\hat{L}_- e^{i\phi} \sin\theta). \quad (1)$$

If $SrFeO_2$ were to have one down-spin electron in the doubly-degenerate level (d_{xz}, d_{yz}), it should have uniaxial magnetic properties with the spin moments parallel to the c axis ($\theta = 0°$) according to the degenerate perturbation theory [10]. Our calculations show that, for the down-spin part, the highest occupied Fe $3d$ level is d_{z^2} while the lowest unoccupied Fe $3d$ level is (d_{xz}, d_{yz}). When the spin lies in the ab plan ($\theta = 90°$), the mixing between d_{z^2} and d_{xz}, d_{yz} due to the raising and lowering operators is the largest. Thus, nondegenerate perturbation theory shows that $SrFeO_2$ has an easy ab- plane anisotropy with a relative large orbital moment.

To explain why the layered compound $SrFeO_2$ has a very high Néel temperature (473 K), we perform MC simulations for a $12 \times 12 \times 12$ supercell based on the classical spin Hamiltonian:

$$H = \sum_{\langle ij \rangle} J_{ij} \vec{S}_i \cdot \vec{S}_j + \sum_i D S_{iz}^2, \quad (2)$$

where the spin exchange parameters J_{ij} are those defined in Fig. 1, $D = 1$ meV (i.e., $DS_{iz}^2 = 4D = 4$ meV) is the spin anisotropy parameter, and $S = 2$. To obtain T_N, we first calculate the specific heat $C = (\langle E^2 \rangle - \langle E \rangle^2)/T^2$ after the system reaches equilibrium at a given temperature (T). Then T_N can be obtained by locating the peak position in the $C(T)$ vs T plot, shown in Fig. 4. For $SrFeO_2$ the calculated T_N is 354 K, which is in reasonable agreement with the experimental value of 473 K. We should note that a smaller U value leads to larger exchange parameters J_1 since $J_1 \propto t^2/U$, and J_2 changes a little; thus, T_N will be higher. For instance, if $U = 4.0$, then $J_1 = 8.68$ meV and $J_2 = 2.23$ meV, resulting in $T_N = 453$ K.

It was shown that large magnetic anisotropy energy can stabilize long-range magnetic order in a one-dimensional (1D) monatomic Co chains [22]. To determine how T_N is affected by the different spin exchange parameters and the spin anisotropy, we performed three additional simulations: one with the spin anisotropy D neglected, one with

TABLE I. Spin exchange parameters (in meV) from the LDA + U calculations. The spin exchange paths J_1, J_2, J_3, and J_4 are defined in Fig. 1. Positive (negative) values indicate that the spin exchange interactions are AFM (FM). For $SrFeO_2$, both the experimental (expt.) [6] and the optimized (opt.) crystal structures were used for the calculations. For $CaFeO_2$ and $BaFeO_2$, the optimized crystal structures were used.

	J_1	J_2	J_3	J_4
$SrFeO_2$ (expt.)	7.04	2.18	0.43	−0.23
$SrFeO_2$ (opt.)	7.91	2.29	0.30	−0.30
$CaFeO_2$ (opt.)	8.90	3.24	0.35	−0.45
$BaFeO_2$ (opt.)	5.81	1.34	−0.29	−0.16

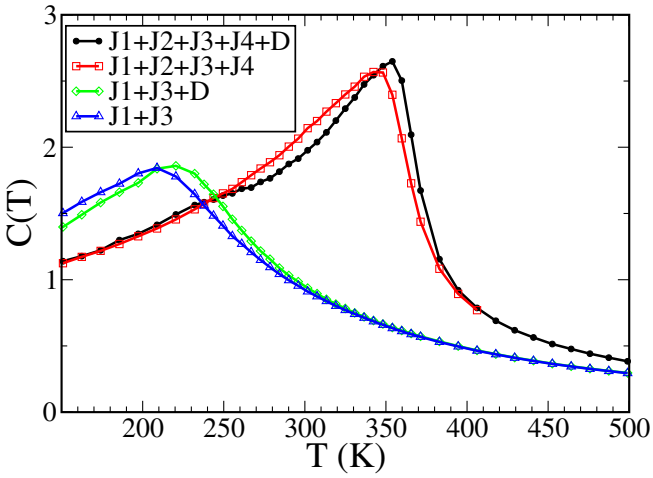

FIG. 4 (color online). Specific heat of $SrFeO_2$, C, calculated as a function of temperature T on the basis of the classical spin Hamiltonian defined in terms of the spin exchange and the spin anisotropy parameters.

the interlayer exchange parameters (J_2 and J_4) neglected, and one with both the interlayer spin exchange parameters (J_2 and J_4) and the spin anisotropy D neglected. The resulting $C(T)$ vs T plots are presented in Fig. 4. As can be seen, when D is disregarded, T_N is only slightly lower (347 K). If only the interlayer exchange parameters are neglected, the $C(T)$ vs T plot shows a broad peak at 220 K. A broad peak occurs at 208 K if both the interlayer exchange parameters and the spin anisotropy are neglected. At any nonzero temperature, a 1D or 2D isotropic Heisenberg model with finite-range exchange interaction can be neither FM nor AFM [23]. Thus, the broad peak in the $C(T)$ vs T plot, obtained when the interlayer spin exchange interactions are neglected, indicates the presence of short-range order. Our MC simulations indicate that the interlayer interactions are primarily responsible for the high T_N of $SrFeO_2$.

It should be noted that $CaFeO_{3-x}$ and $BaFeO_{3-x}$ have structures and properties similar to those of $SrFeO_{3-x}$. Thus, it is of interest to consider the structural and magnetic properties of hypothetical $CaFeO_2$ and $BaFeO_2$ assuming that they are isostructural with $SrFeO_2$. For this purpose, the structures of $MFeO_2$ (M = Sr, Ca, Ba) were optimized by performing LDA + U calculations for the AF1 state. The optimized lattice constants a and c for $SrFeO_2$ are 3.92 and 3.40 Å, respectively, which are in good agreement with experiment. The calculated lattice constants are $a = 3.86$ Å and $c = 3.12$ Å for $CaFeO_2$, and $a = 3.98$ Å and $c = 3.79$ Å for $BaFeO_2$. The trend in the lattice constants is consistent with the ionic radii of Ca^{2+}, Sr^{2+}, and Ba^{2+}. The exchange parameters calculated for the optimized $MFeO_2$ (M = Sr, Ca, Ba) structures are listed in Table I. All these compounds should have the AF1 state as the ground state since the spin exchange interactions are dominated by AFM J_1 and J_2. Among $MFeO_2$ ($M = Ca$, Sr, Ba), $CaFeO_2$ has the largest J_1 and J_2 values, while $BaFeO_2$ has the smallest J_1 and J_2 values. This trend reflects the fact that the strengths of these interactions increase with decreasing the lattice constants. Thus, $CaFeO_2$ is predicted to have a higher T_N than does $SrFeO_2$.

In summary, $SrFeO_2$ has no Jahn-Teller instability because the occupied down-spin d level is d_{z^2}. The Néel temperature of $SrFeO_2$ is high because the intralayer NN spin exchange is strong while the interlayer NN spin exchange is substantial. The in-plane magnetic anisotropy of $SrFeO_2$ arises from the SOC-induced interaction between the d_{z^2} and (d_{xz}, d_{yz}) states.

Work at NREL was supported by the U.S. Department of Energy, under Contract No. DE-AC36-99GO10337. The research at NCSU was supported by the Office of Basic Energy Sciences, Division of Materials Sciences, U.S. Department of Energy, under Grant No. DE-FG02-86ER45259.

[1] Z. Shao and S. M. Haile, Nature (London) **431**, 170 (2004).
[2] H. Falcón *et al.*, Chem. Mater. **14**, 2325 (2002).
[3] S. P. S. Badwal and F. T. Ciacchi, Adv. Mater. **13**, 993 (2001).
[4] Y. Wang *et al.*, Mater. Lett. **49**, 361 (2001).
[5] A. Lebon *et al.*, Phys. Rev. Lett. **92**, 037202 (2004).
[6] Y. Tsujimoto *et al.*, Nature (London) **450**, 1062 (2007).
[7] M. A. Hayward and M. J. Rosseinsky, Nature (London) **450**, 960 (2007).
[8] A. F. Wells, *Structural Inorganic Chemistry* (Oxford University Press, Oxford, U.K., 1962), 3rd ed.
[9] Y. Murakami *et al.*, Phys. Rev. Lett. **81**, 582 (1998).
[10] D. Dai and M.-H. Whangbo, Inorg. Chem. **44**, 4407 (2005).
[11] P. E. Blöchl, Phys. Rev. B **50**, 17 953 (1994); G. Kresse and D. Joubert, *ibid.* **59**, 1758 (1999).
[12] G. Kresse and J. Furthmüller, Comput. Mater. Sci. **6**, 15 (1996); Phys. Rev. B **54**, 11 169 (1996).
[13] J. P. Perdew and A. Zunger, Phys. Rev. B **23**, 5048 (1981); D. M. Ceperley and B. J. Alder, Phys. Rev. Lett. **45**, 566 (1980).
[14] A. I. Liechtenstein *et al.*, Phys. Rev. B **52**, R5467 (1995).
[15] H. J. Xiang and M.-H. Whangbo, Phys. Rev. Lett. **98**, 246403 (2007).
[16] G. M. Dalpian *et al.*, Solid State Commun. **138**, 353 (2006).
[17] H. J. Xiang, C. Lee, and M.-H. Whangbo, Phys. Rev. B **76**, 220411(R) (2007).
[18] J. Kanamori, J. Phys. Chem. Solids **10**, 87 (1959).
[19] J. B. Goodenough, Phys. Rev. **100**, 564 (1955).
[20] H. J. Xiang and M.-H. Whangbo, Phys. Rev. B **75**, 052407 (2007).
[21] X. Wang *et al.*, Phys. Rev. B **54**, 61 (1996).
[22] P. Gambardella *et al.*, Nature (London) **416**, 301 (2002).
[23] N. D. Mermin and H. Wagner, Phys. Rev. Lett. **17**, 1133 (1966).